Structural phase diagram, magnetism, and exchange-biased behavior of Fe films on Fe$_x$Mn$_{1-x}$/Cu(001)

Wei Pan,[1,2,*] Wen-Chin Lin,[2,3] Nai-Yeou Jih,[2] Cheng-Hau Chuang,[2] Yu-Chun Chen,[2] Chien-Cheng Kuo,[2,4]
Po-Chun Huang,[2] and Minn-Tsong Lin[2,3,†]

[1]*Department of Physics, National Chung Cheng University, Chia-Yi 621, Taiwan*
[2]*Department of Physics, National Taiwan University, Taipei 106, Taiwan*
[3]*Institute of Atomic and Molecular Sciences, Academia Sinica, Taipei 106, Taiwan*
[4]*Department of Physics, National Sun Yat-Sen University, Kaohsiung 804, Taiwan*
(Received 11 May 2006; published 26 December 2006)

The fcc-bcc structural phase transition and the interlayer exchange-bias coupling in a Fe/Fe$_x$Mn$_{1-x}$/Cu(001) system are studied in a wide x range with different growth temperatures. For depositions of Fe at 150 K on the Fe$_x$Mn$_{1-x}$ layer with $x < 0.35$, the transition occurs below 15 ML and the resulting bcc Fe films are ferromagnetic with exchange bias. The fcc Fe is stabilized up to 20 and 25 ML for the depositions on the Fe$_x$Mn$_{1-x}$ layer with $x > 0.35$ at 150 and 300 K, respectively. Both fcc Fe films show no magnetic signal. The relation comprising the structure and magnetic coupling of the Fe films might be attributed to the x-dependent interface roughness at Fe/Fe$_x$Mn$_{1-x}$.

I. INTRODUCTION

For understanding the physical origin of the nanomagnetic phenomena, correlations of structure and magnetism in nanoscale become more important. The structure variation can be achieved by molecular-beam epitaxy techniques, i.e., depositions of films on a substrate with proper lattice constant and surface orientation. In reduced dimensional system, e.g., ultrathin films, the magnetic property may behave very differently from that of the bulk. It is strongly correlated to the surface conditions, lattice strain, alloy composition, the growth conditions, and the roughness at the interphase between film and substrate.[1–6] A typical model is the magnetic phase of the face-centered cubic (fcc) Fe, which exits between 1184 and 1664 K (Curie temperature=1043 K). The magnetic phases of the fcc Fe films are sensitive to the atomic volume, tetragonal distortion, growth condition, and surface reconstruction because the ferromagnetic (FM), antiferromagnetic (AF), and paramagnetic phases are energetically close.[7–14]

Several fcc substrates have been introduced to provide templates with different lattice constants, e.g., Cu(001) (a=3.61 Å),[8–11,15] Ni(001)/Cu(001), Co(001)/Cu(001),[16] Cu$_3$Au (a=3.75 Å),[17] Cu$_{90}$Au$_{10}$ (a=3.66 Å),[18] and Cu$_{84}$Al$_{16}$ (a=3.65 Å).[19] The structure and magnetic properties for the depositions of Fe on Cu(001) at room temperature in several studies[8–11] are summarized as follows: (i) Face-centered tetragonal (fct) structure corresponds to out-of-plane magnetization for the films below four monolayers (ML), (ii) face-centered cubic (fcc) structure with two fct overlayers corresponds to out-of-plane magnetization with a constant magnetic remanence for the films in 4–11 ML, and (iii) body-centered cubic (bcc) structure accompanied with in-plane magnetization for the films above 12 ML.[8,10,11] The results of the depositions of Fe on other substrates mentioned above are similar to that of Fe on Cu(001). The bcc structure associated with the ferromagnetic (FM) phase agrees both in the experiments and the theoretical prediction.[13] Recently, the explanation of the FM ordering for the Fe/Cu(001) films

below 10 ML [regimes (i) and (ii)] is challenged. A nanomartensitic $(1 \times n)$ bcc nucleation center is observed on the surface of 2–4 ML Fe/Cu(100) by using low energy electron diffraction (LEED) (Ref. 20) or scanning tunneling microscopy (STM) (Ref. 21) with atomic resolution. This bcc-like surface reconstruction was suggested to be the origin of the FM ordering of the fcc-fct mixed superstructure phase.[10,22] Another study by using spin-resolved inverse photoemission reported that the FM ordering of the fcc-fct mixed phase was not only restricted on the topmost layer but also found in sublayers with reduced magnetic moment.[23] A strong correlation between the FM phase and the bcc-like reconstruction induced by the shear instability was also indicated by Spišák and Hafner in a theoretical work by *ab initio* local-spin-density calculations.[14] The existence of the bcc-like film was also suggested to be extremely sensitive to any effect influencing the energy balance.[22] To clarify the correlation of the structure magnetism of Fe films, a single fcc Fe structure is demanded.

In this article, we introduce Fe$_x$Mn$_{1-x}$ layers between Fe films and the Cu(001) substrate to clarify this structure-magnetism correlation of Fe. The lattice constant and Fe$_x$Mn$_{1-x}$ alloys exhibit compositional dependence, which varies from 3.796 to 3.605 Å as the composition x increases.[24] Additionally, the AF configuration of Fe$_x$Mn$_{1-x}$ alloys changes from collinear along the long axis, 3Q, and collinear along the long axis as the composition x increases.[24–31] Thus varying the composition x effectively varies the lattice mismatch between the Fe$_x$Mn$_{1-x}$ layer and Cu(001) as well as the corresponding AF configuration. We observe that the structure of Fe films on 17 ML Fe$_{0.5}$Mn$_{0.5}$/Cu(001) is single fcc structure up to 20 ML grown at 150 K and 25 ML at 300 K. The compositional dependence of the surface roughness of the Fe$_x$Mn$_{1-x}$ layer as well as the critical thickness (t_c) for fcc-bcc structural transition of the Fe overlayer will be shown in this paper. The correlation of the stabilization of the fcc structure and the interface roughness of the Fe$_x$Mn$_{1-x}$ layer will be discussed.

II. EXPERIMENT

The experiment was performed in an ultrahigh vacuum chamber (UHV) with a base pressure below 2×10^{-10} mbar. The substrate is a Cu(001) disk with a thickness of 2 mm and diameter of 10 mm. The surface was cleaned by Ar^+ sputtering in the energy of 2 keV at the pressure of 5×10^{-5} mbar and checked by Auger electron spectroscopy (AES) for cleanliness. The crystalline structure was rebuilt by annealing to 790 K within 30 min followed by keeping at 805 K for 10 min. The structure was checked by the sharp 1×1 pattern shown in low energy electron diffraction (LEED) indicating a good crystalline ordering. The Fe_xMn_{1-x} alloy films on Cu(001) were prepared by thermal co-deposition of Fe (99.999 at. %) and Mn (99.995 at. %) at 300 K, and followed by deposition of Fe at 150 or 300 K. The growth of the film was monitored by medium energy electron diffraction (MEED). The incident electron beam is along [010] orientation in azimuth with an angle of 2° with respect to the surface. The maximum of the specular (00) MEED intensity indicating the filled layer allows us to determine the thickness within an accuracy of ±0.1 ML. The deposition rate for the Fe_xMn_{1-x} and the following Fe films is adjusted to approximately 0.8 ML and 0.5 ML per minute, respectively. The chemical composition x of the Fe_xMn_{1-x} alloy films was adjusted by the individual deposition rate of Fe and Mn as well as calibrated by AES. The compositional accuracy of 3% (0.03) of Fe_xMn_{1-x} films was obtained by controlling the evaporation rate precisely with a codeposition technique.[32] It is achieved through keeping both the emission and monitor (ion) current constant during depositions by tuning the filament current of an evaporation gun (OMICRON EFM-3) with the assistance of a feedback circuit.[1,5] It is, however, more difficult to control the deposition rate for Mn[28,34] than that for Fe, Co, and Ni. The crystalline ordering was characterized by the LEED pattern. The average vertical interlayer distance d was obtained by the kinematic analysis on specular intensity curves in $I(E)$ LEED with a series of periodic intensity maxima referring to the Bragg condition,

$$d = \frac{n\pi\hbar}{\sqrt{8m(E + V_0)}\cos\theta}, \quad (1)$$

where n, θ (5°), m, E, and V_0 are noted for the order of interference, incident angle of the electron beam, electron mass, primary electron energy, and inner potential energy, respectively. The statistical error was obtained by taking the root mean square of the fitted data. By this method, the error of d was restricted within ±0.01 Å. Additionally, the periodicity of the lattice near the surface is recognized by a series of the intensity maxima of the LEED-$I(E)$ curves, such that the single fcc, fcc-fct, or bcc structure is distinguished. This technique has been successfully applied to resolve the average structural information to understand the interrelation between magnetic properties and the lattice parameter in many previous studies.[1,11,17,33,35] The lateral interlayer distance was extracted from the distance between spots of the LEED pattern, however with a larger error around 0.03 Å due to diffusion of the diffraction spots. For consistency, all LEED pattern and LEED-$I(E)$ curves were taken at 200 K.
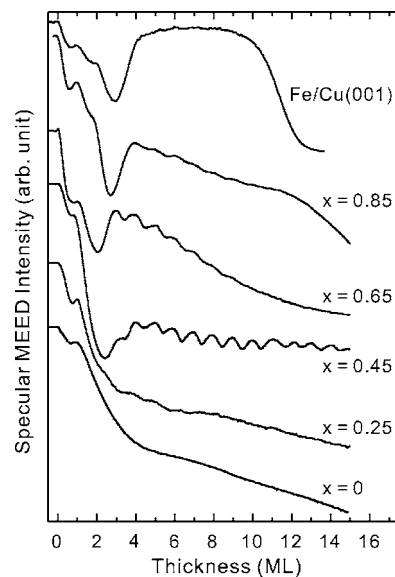

FIG. 1. Specular (00) MEED intensity as a function of thickness during deposition of Fe_xMn_{1-x} on Cu(001) at 300 K with different composition x. The oscillatory behavior shows compositional dependence. The oscillations are pronounced for $0.45 < x < 0.65$, which indicates a layer-by-layer growth mode. The drastic decrease in the MEED intensity as Fe/Cu(001) is not observed in the curves for the Fe_xMn_{1-x} films, which indicates that the fcc-bcc transition does not occur in the thickness range investigated.

The surface morphology of Fe films on Cu(001) or Fe_xMn_{1-x}/Cu(001) and Fe_xMn_{1-x}/Cu(001) were characterized by a scanning tunnelling microscope (STM) in UHV environment. The STM images shown in the figures were taken under the constant current mode at 300 K (RT) with the current and the voltage as noted in the captions.

The magnetic property was measured by *in situ* dynamic magneto-optical Kerr effect (MOKE) both in in-plane and out-of-plane orientation at temperatures ranging from 110 to 330 K. The lock-in technique is applied in MOKE, which allows the intensity of the Kerr signal to be normalized. One can obtain the coercivity (H_c) and exchange-bias field (H_{ex}) as well as the relative remanence (M_r) and saturated magnetic signal (M_s) from the hysteresis loops. For observing the exchange bias phenomenon, the films were cooled from 300 to 90 K under a magnetic field of 350 Oe at in-plane or out-of-plane direction with respect to the following MOKE measurements. Details of the experiments can be found in our previous works.[5,33,36]

III. RESULT

A. Growth and the fcc structure of Fe_xMn_{1-x} on Cu(001)

The growth of Fe_xMn_{1-x} alloy films on Cu(001) was monitored by specular (00) MEED intensity during depositions. The curves as a function of thickness for various composition x are shown in Fig. 1. The growth mode of Fe_xMn_{1-x} alloy films exhibits compositional dependence. For Mn-rich Fe_xMn_{1-x} alloy films where $x < 0.3$, only one peak is found in the initial growth which followed by decline of the
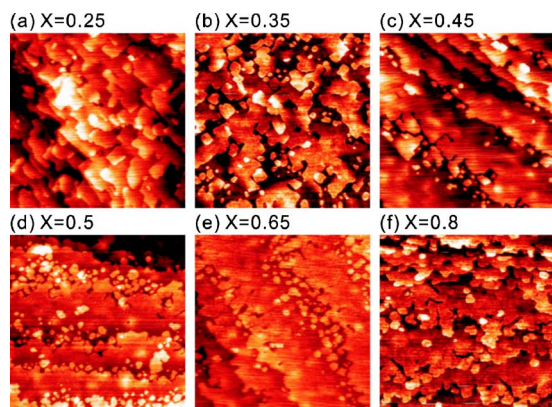
FIG. 2. (Color online) Surface morphology taken by STM for 17 ML Fe_xMn_{1-x}/Cu(001) with $x=0.25$, 0.35, 0.45, 0.50, 0.65, and 0.80 as labeled above. The terraces on the surface of Fe_xMn_{1-x} with composition x close to 0.5 are larger than those on either the Fe rich or Mn rich alloy films. The dimension for each STM image is 200×200 nm². These images were taken under the constant current mode at room temperature. The tunneling current and the bias voltage for the images are (a) 1.752 nA and 0.18 V, (b) 0.8 nA and 1.8 V, (c) 3.0 nA and 0.5 V, (d) 0.8 nA and −1.5 V, (e) 30 nA and 0.5 V, and (f) 0.3 nA and 1.0 V, respectively.

intensity. For Fe-rich Fe_xMn_{1-x} alloy films where $x>0.8$, the MEED curve shows an Fe-like growth fashion such that the layered oscillations are found in the first two layers and followed by an intensity minimum at the thickness of 3 ML. Nevertheless, the curves show mild oscillations for the thickness in excess of 4 ML but no drastic intensity decline at 10 ML as the curve for Fe/Cu(001). It indicates no fcc-bcc phase transition occurs in this thickness range. For the films with x between 0.45 to 0.65, the curves show pronounced oscillations with a period of one atomic layer for the coverage in excess of 4 ML. A layer-by-layer growth mode is found in this composition range, which demonstrates a very different fashion from either the Fe-rich or Mn-rich Fe_xMn_{1-x} alloy films. The coherent oscillations of both stress and MEED curves in a previous study on the growth of $Fe_{0.5}Mn_{0.5}$/Cu(001) indicates that the Fe_xMn_{1-x} alloy films tend to wet the surface.[36] The missing oscillation in the MEED curves for the initial growth of Fe_xMn_{1-x} is ascribed to the formation of the $c(2 \times 2)$ MnCu surface alloy due to an Mn-Cu atomic exchange mechanism.[37] This MnCu surface alloy formation leads to a deviation in composition of the Fe_xMn_{1-x} alloy films near the FeMn-Cu interface. For avoiding the compositional and structural instability near the FeMn-Cu interface, the thickness of the Fe_xMn_{1-x} layer is thus chosen to be 17 ML, which is also for the enhancement of the Néel temperature (T_N) owing to the finite size effect.

B. Surface roughness and strain of 17 ML Fe_xMn_{1-x}/Cu(001)

Figure 2 shows the STM images of 17 ML Fe_xMn_{1-x}/Cu(001) with $x=0.25$, 0.35, 0.45, 0.50, 0.65, and 0.8. The dimension of the images is 200×200 nm². The STM images show that the surfaces of 17 ML Fe_xMn_{1-x}/Cu(001) with x
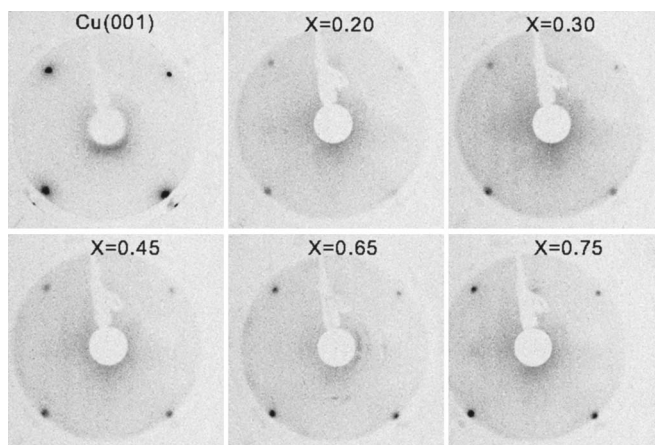

FIG. 3. LEED patterns taken at 44 eV for Cu(001) substrate and 17 ML Fe_xMn_{1-x}/Cu(001) with different composition (see labels). Only the (1×1) LEED pattern is observed for the Fe_xMn_{1-x} films, which indicates a good fcc crystalline ordering as the Cu(001) surface.

between 0.45 to 0.65 are smoother than the composition either below or in excess of this composition range. From the STM images, the surface roughness indicated by root mean square of the height is 1.95 and 1.38 Å for $x=0.50$ and 0.65, respectively, whereas it is 4.98 Å for $x=0.25$.

LEED patterns for the 17 ML Fe_xMn_{1-x} films with different x are shown in Fig. 3. Although no distinct oscillations are observed in the MEED curves for the films with x below 0.3, the (1×1) LEED pattern is found as that of the Cu(001) substrate. It indicates that no superstructure or reconstruction occurs on the surfaces of 17 ML Fe_xMn_{1-x} films.

Comparing the STM images and the MEED data in Fig. 1, one can conclude that the layer-by-layered oscillations in MEED curves refer to a smooth surface. In other words, the surfaces of the Fe-rich or Mn-rich Fe_xMn_{1-x}/Cu(001) films are relatively rougher whereas the lattices remain on fcc sites.

The surface roughness is an efficient way to release the stress induced by the strain of the film. Although the elastic property of Fe_xMn_{1-x} with different x is not available, one can obtain the stress state qualitatively by deducing the lattice mismatch between the Fe_xMn_{1-x} alloys and the Cu(001) substrate. The lattice constant of the bulk Fe_xMn_{1-x} is obtained from the study by Endoh and Ishikawa.[24] The lattice mismatch η between bulk Fe_xMn_{1-x} alloys and Cu(001) ranges from −0.14% to 5.1% by the definition that $\eta=(a_{Cu}-a_{FeMn})/a_{FeMn}$, where $a_{Cu}=3.610$ Å. The composition of bulk Fe_xMn_{1-x} alloys corresponding to the least mismatch is about 0.5, where the Fe_xMn_{1-x} films are less strained. The interlayer distance of the 17 ML Fe_xMn_{1-x}/Cu(001) derived from LEED-$I(E)$ and the bulk Fe_xMn_{1-x} (Ref. 24) are shown in Fig. 4. The discrepancy of the solid and dashed lines indicates the strain state of the Fe_xMn_{1-x} alloy films. The most strained Fe_xMn_{1-x} films are those films with low x, the Mn-rich Fe_xMn_{1-x} alloys for the large η. Thus the strain state and the surface roughness of the film are correlated so that the strain may increase the surface roughness for the Fe_xMn_{1-x}/Cu(001) films.
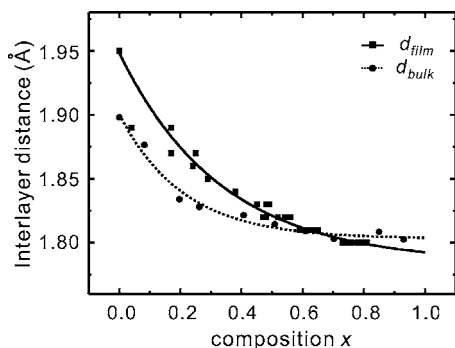
FIG. 4. The interlayer distance for the bulks and films of the Fe_xMn_{1-x} alloy as a function of the composition x. The films with Mn-rich ($x \lesssim 0.4$) composition are more strained than the films with equiatomic composition ($x \sim 0.5$). The data for the films are obtained by the kinetic analysis of the $I(E)$ LEED curves and the bulks are from Ref. 24. The lines are guides for the eyes.

C. Single fcc structure and fcc-bcc transition of Fe films on 17 ML Fe_xMn_{1-x}/Cu(001)

The structure of Fe films on 17 ML Fe_xMn_{1-x}/Cu(001) is investigated by LEED, LEED-$I(E)$, and MEED studies. LEED patterns and the LEED-$I(E)$ curves for 15 ML and 3 ML Fe grown on 17 ML $Fe_{0.5}Mn_{0.5}$/Cu(100) and 3 ML Fe/Cu(100) are shown in Figs. 5(a)–5(c), respectively. For 3 ML Fe/Cu(100) as shown in Fig. 5(c), the LEED $I(E)$ curve shows two distinct sets of intensity maxima indicating fcc and fct structure with the interlayer distance d of 1.84 and 1.95 Å, respectively. The LEED pattern shows a (1×4) ordering, which agrees with the previous study.[10] Only single fcc structure is observed for the Fe films on 17 ML Fe_xMn_{1-x}/Cu(001) in this thickness range. Selected LEED $I(E)$ curves as shown in Figs. 5(a) and 5(b) exhibit only one set of intensity maxima indicating fcc structure associated with a (1×1) ordering in the LEED pattern. No indication of fcc-fct mixed phase is found in the LEED-$I(E)$ curves of Fe films on 17 ML Fe_xMn_{1-x}/Cu(001) as shown Fig. 5. One can conclude that the structure of Fe films (3 to 15 ML) on 17 ML Fe_xMn_{1-x}/Cu(001) is single fcc phase, whereas the structure of Fe/Cu(001) near the interphase is mixed fcc-fct structure.

For Fe/Cu(001) films ($x = 1$ in Fig. 1), the drastic decrease of the MEED intensity at 10 ML indicates the fcc-bcc structural transition owing to the rough bcc(011) surface.[38] It implies that the specular (00) MEED intensity curves during deposition of Fe films provide not only the information of the growth mode but also the critical thickness t_c for the fcc-bcc structural transition. An experiment to analyze the fcc-bcc structural phase transition by combining MEED and LEED-$I(E)$ was performed. The specular (00) MEED intensity as a function of thickness for Fe deposition on 17 ML $Fe_{0.5}Mn_{0.5}$/Cu(001) at 300 K and the LEED-$I(E)$ curves taken at different thicknesses are shown in Figs. 6(a) and 6(b), respectively.

The LEED-$I(E)$ curve for FeMn/Cu(001) films provides a model curve to identify the fcc structure. From the series of intensity maxima denoted by the solid lines, an interlayer
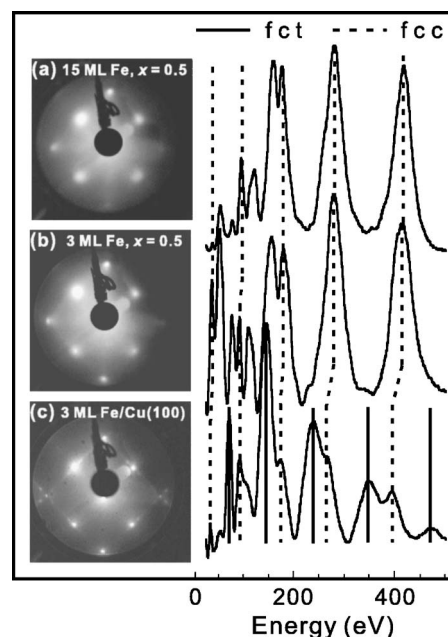

FIG. 5. LEED pattern taken at 115 eV and LEED $I(E)$ curves for (a) 15 ML Fe on 17 ML $Fe_{0.50}Mn_{0.50}$/Cu(100), (b) 3 ML Fe on 17 ML $Fe_{0.50}Mn_{0.50}$/Cu(100), and (c) 3 ML Fe on Cu(100). The solid and dashed lines indicate the characteristic peaks for fct and fcc structure, respectively. A single fcc phase is observed up to 15 ML for Fe films grown on 17 ML $Fe_{0.50}Mn_{0.50}$/Cu(100) accompanying an (1×1) ordering in the LEED pattern. A fct-fcc mixed phase is found for 3 ML Fe on Cu(100) accompanying a (1×4) ordering in the LEED pattern.

distance of 1.81 Å indicating fcc structure is obtained. Thus one can recognize the fcc structure by the solid lines in Fig. 6(b). Another interlayer distance of 2.02 Å is calculated from the LEED-$I(E)$ curves for 33 ML Fe/17 ML $Fe_{0.5}Mn_{0.5}$/Cu(001) in Fig. 6(b). This distance indicates that the surface of film is bcc(011). Thus the bcc structure can be characterized from the LEED-$I(E)$ curves as denoted by the dashed lines in Fig. 6(b). Below 27 ML, the structure of Fe films is fcc indicated by the LEED-$I(E)$ curve, which shows the same series of intensity maxima as the LEED-$I(E)$ curves for the $Fe_{0.5}Mn_{0.5}$ alloy film. An additional series of intensity maxima for the bcc structure is found in the LEED-$I(E)$ curves of 30 ML Fe films, which indicates an fcc-bcc mixed phase in this thickness regime. For 33 ML Fe/17 ML $Fe_{0.5}Mn_{0.5}$/Cu(001), only a characteristic LEED-$I(E)$ curve for bcc structure that corresponds to the drastic decrease in the MEED intensity curve is found. It indicates the fcc-bcc structural transition occurs in the thickness regime between 30 and 33 ML. The drastic decrease in the MEED intensity curve provides us with an estimation of the t_c for the fcc-bcc structural transition of the Fe films deposited on Fe_xMn_{1-x} alloys. Another result from the MEED curves for deposition of Fe on Fe_xMn_{1-x}/Cu(001) is the significant oscillations in the first few layers, which are very different from the MEED curve for the depositions of Fe on Cu(001) as shown in Fig. 1. The MEED curve for Fe on $Fe_{0.5}Mn_{0.5}$/Cu(001) shows layer-by-layer oscillations up to 13 ML (see the MEED curve in Fig. 7 as well), whereas the curve for Fe/Cu(001) drops
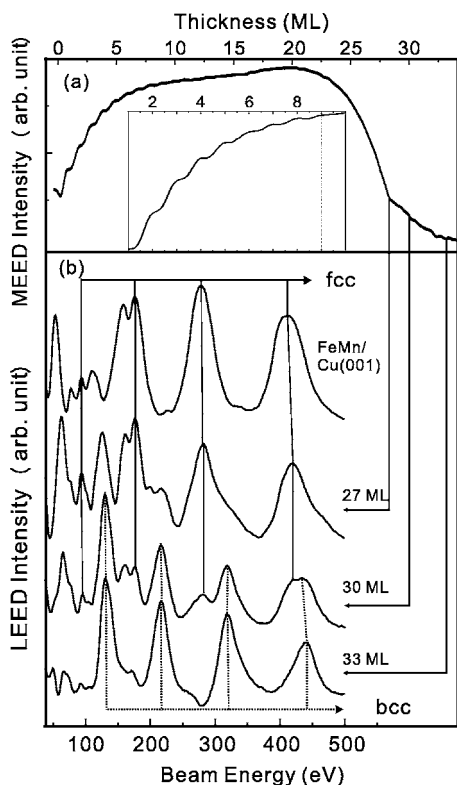
FIG. 6. $I(E)$ LEED curves taken at different stages of the decrease in the specular MEED intensity curve. (a) The specular MEED intensity during the deposition of the Fe on 17 ML $Fe_{0.5}Mn_{0.5}/Cu(001)$ at 300 K. (b) $I(E)$ LEED taken at the thickness indicated by the arrows. Solid and dotted lines indicate the characteristic peaks for the fcc and bcc phase, respectively. Enlarged MEED curve from the first to the tenth ML is shown in the inset. Single fcc phase as the $Fe_{0.5}Mn_{0.5}/Cu(001)$ is observed below 27 ML corresponding to the middle stage of decrease in the MEED curve. It becomes an fcc-bcc mixed phase between 27 to 33 ML and a bcc phase at 35 ML, which corresponds to the final stage in the MEED curve. The drastic decrease of the MEED curve indicates the fcc-bcc phase transition for the Fe films during deposition.

down during the first three layers that followed by increasing in intensity at the coverage around 4 ML, indicating the fct-fcc mixed structure. It implies that the fcc-fct mixed structure during deposition of Fe on the Fe_xMn_{1-x} layer is absent. Additionally, in contrast to the MEED curve for Fe/Cu(001), the MEED intensity for Fe on $Fe_xMn_{1-x}/Cu(001)$ increases after depositing Fe upon the Fe_xMn_{1-x} layer. This indicates significant improvement on the film surface.

The effect of Fe growth temperature and composition x of 17 ML Fe_xMn_{1-x} to the t_c for the fcc-bcc structural transition is studied by the MEED study as shown in Fig. 7. For Fe films on 17 ML $Fe_{0.5}Mn_{0.5}/Cu(001)$ grown at 150 and 300 K, the t_c is 20 and 25 ML, respectively. The fcc structure is stabilized at higher deposition temperature. The t_c is affected by the x of 17 ML $Fe_xMn_{1-x}/Cu(001)$. At 150 K, it ranges from 12 to 20 ML while x varies from 0.3 to 0.5.

The structural phase of Fe films deposited on 17 ML $Fe_xMn_{1-x}/Cu(001)$ at 150 K is summarized in Fig. 8. The fcc or bcc structure characterized by LEED-$I(E)$ is labeled by blank ($\bigcirc$) or filled ($\bullet$) circles, respectively. The t_c for
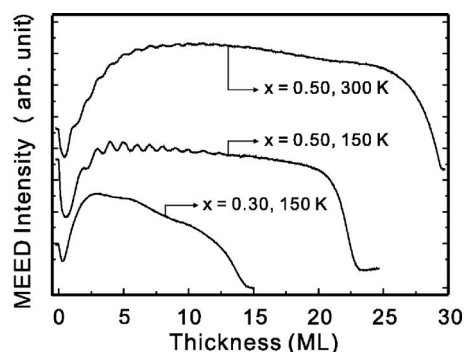

FIG. 7. Specular MEED intensity during deposition as a function of film thickness for Fe films on $Fe_xMn_{1-x}/Cu(100)$ with x =0.3 and 0.5 at 150 or 300 K. For Fe films grown at 300 K, t_c of fcc-bcc transition is shifted from 12 to 25 ML by the $Fe_{0.50}Mn_{0.50}$ buffer layer. On the $Fe_{0.50}Mn_{0.50}$ layer, t_c is shifted from 20 to 25 ML by increasing the growth temperature from 150 to 300 K. At 150 K, t_c varies from 12 to 20 ML by adjusting x of the Fe_xMn_{1-x} buffer layer from 0.30 to 0.50.

fcc-bcc structural transition characterized by the drastic drop of the MEED curve is labeled by +. The t_c reaches maximum for the Fe films grown on 17 ML $Fe_xMn_{1-x}/Cu(001)$ with x near 0.5 and decreases for the Fe films grown on an Fe-rich or Mn-rich Fe_xMn_{1-x} buffer layer.

The contribution of Fe_xMn_{1-x} films on the surface morphology of Fe films was investigated by STM. The STM images and roughness by line scan on the images for 15 ML Fe films with (left) or without (right) 17 ML $Fe_{0.5}Mn_{0.5}$ interlayer are shown in Fig. 9. The roughness is nearly 2 Å (equivalent to 1 ML) for the Fe films with a 17 ML $Fe_{0.5}Mn_{0.5}$ interlayer, whereas it is 12 Å (equivalent to 6 ML) for the films without the interlayer. The surface roughness of the Fe film is highly reduced while depositing on 17 ML $Fe_{0.5}Mn_{0.5}$. Summarizing the STM, LEED-$I(E)$, and MEED studies, it suggests a stabilization of the fcc phase of Fe films for the depositions on 17 ML Fe_xMn_{1-x} with x ranging from

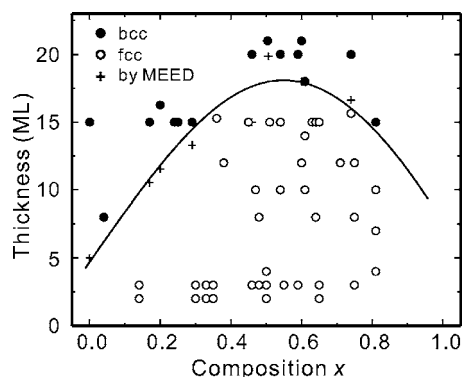FIG. 8. The compositional dependence of the t_c for the fcc-bcc transition of the Fe films grown on 17 ML $Fe_xMn_{1-x}/Cu(001)$ at 150 K. The structural phase transition characterized by $I(E)$ LEED analysis is denoted by blank ($\bigcirc$) or filled ($\bullet$) circles, and the transition characterized by the drastic decrease in the MEED intensity curve during deposition is denoted by a + sign. The t_c reaches 20 ML for the Fe films grown on $Fe_{0.5}Mn_{0.5}$ and decreases on either Fe-rich or Mn-rich films.
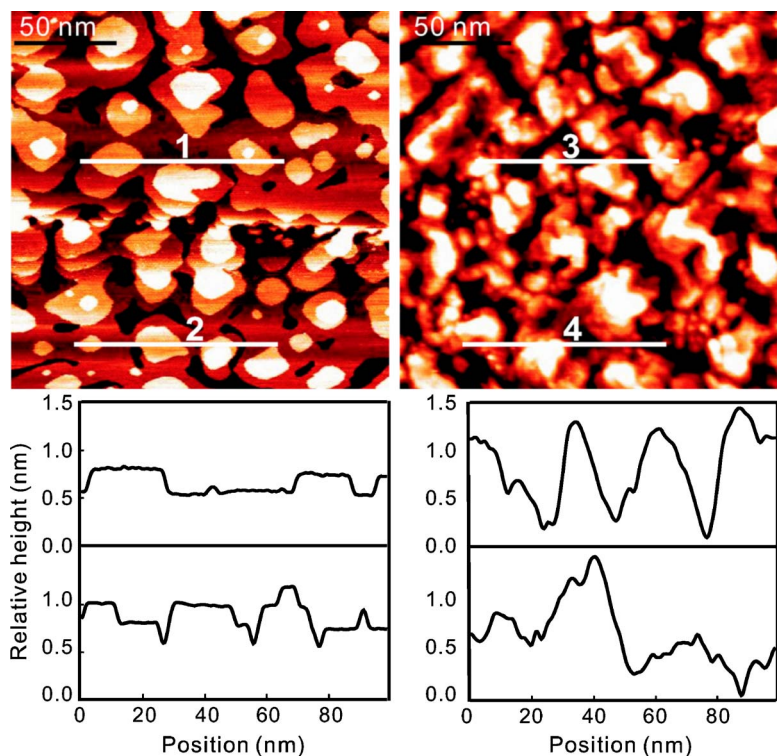
FIG. 9. (Color online) Surface morphology taken by STM and roughness by line scan for 15 ML Fe/17 ML $Fe_{0.5}Mn_{0.5}$/Cu(001) (left) and 15 ML/Cu(001) (right). The surface roughness of Fe films is reduced significantly by introducing the $Fe_{0.5}Mn_{0.5}$ alloy films. The images were taken under the constant current mode at room temperature. The tunneling current and the bias voltage are 1.0 nA and 2.0 V for 15 ML Fe/17 ML $Fe_{0.5}Mn_{0.5}$/Cu(001) and 0.8 nA and 2.0 V for 15 ML/Cu(001), respectively.

0.4 to 0.7. Note that the composition range coincides with the range of Fe_xMn_{1-x}/Cu(001) with less surface roughness as shown in Fig. 2. It implies that the smooth surface of Fe_xMn_{1-x}/Cu(001) stabilizes the fcc structure of Fe films.

D. Magnetic property and exchange bias of Fe on Fe_xMn_{1-x}/Cu(001)

To clarify the structure-magnetism correlation, deposition of 15 ML Fe on 17 ML Fe_xMn_{1-x}/Cu(001) was performed in a wide composition range: $0 < x < 0.82$. All MOKE hysteresis loops shown in Figs. 10–12 are taken in longitudinal geometry. No MOKE signal is found in out-of-plane orientation. The MOKE hysteresis loops measured with increase of temperature after field cooling for the 15 ML Fe films

deposited on 17 ML Mn/Cu(001) ($x=0$) are shown in Fig. 10. No exchange bias is found. The coercivity (H_c) decreases from 13 Oe to 8 Oe as the temperature increases from 110 to 300 K. The bcc Fe films exhibit typical ferromagnetic property. The loops for the Fe films deposited on 17 ML Fe_xMn_{1-x}/Cu(001) with $x=0.2$ and 0.3 are shown in Fig. 11 and Fig. 12, respectively. A negative exchange-bias coupling is found in both cases. The H_c of Fe films is largely enhanced in a factor of 10 by the exchange-biased coupling compared to that of the Fe films on 17 ML Mn/Cu(001). The exchange-bias coupling exhibits two different types of temperature-dependent behavior. For both films, the exchange bias field (H_{ex}) is −40 Oe at 150 K, which increases along the temperature and approaches zero at about 270 K [the blocking temperature (T_b)]. For the Fe film grown on
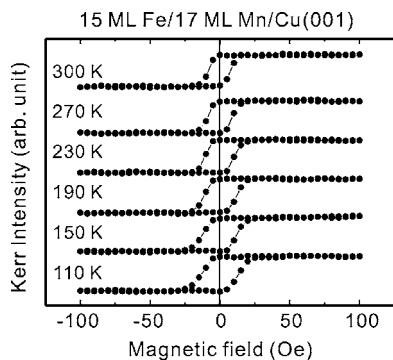

FIG. 10. Magnetic hysteresis loops taken by longitudinal MOKE at different temperatures after field cooling for 15 ML Fe/17 ML Mn/Cu(001) [regime (I) of Fig. 13]. No exchange-bias coupling is observed in the temperature range investigated. The H_c is about 12 Oe at 150 K.
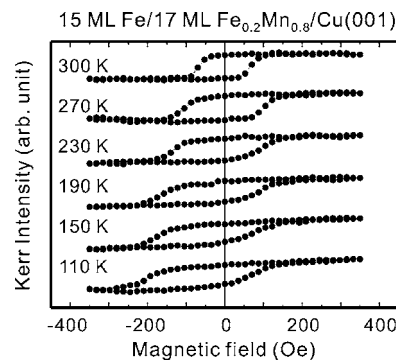

FIG. 11. Magnetic hysteresis loops taken by longitudinal MOKE at different temperatures after field cooling for the 15 ML Fe/17 ML $Fe_{0.2}Mn_{0.8}$/Cu(001) [regime (II) of Fig. 13]. The exchange-bias coupling with enhanced H_c is found. The H_{ex} =−40 Oe with H_c of 116 Oe is observed at 150 K.
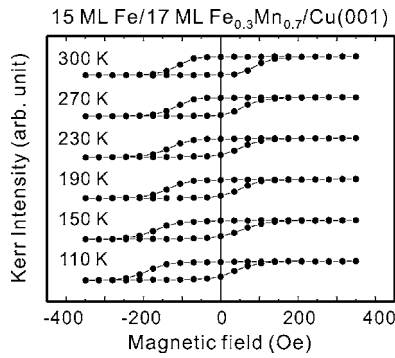
FIG. 12. Magnetic hysteresis loops taken by longitudinal MOKE at different temperatures after field cooling for the 15 ML Fe/17 ML $Fe_{0.3}Mn_{0.7}$/Cu(001) [regime (II) of Fig. 13]. An exchange-bias coupling with enhanced H_c is found. $H_{ex} = -40$ Oe with H_c of 94 Oe is observed at 150 K.

Fe_xMn_{1-x} with $x = 0.2$, the H_c decreases monotonically along with the temperature increases. For the Fe film grown on Fe_xMn_{1-x} with $x = 0.3$, the H_c decreases but is enhanced while the H_{ex} approaches zero, the so-called peak effect.[39,40] This phenomenon has been discussed in our previous publication.[43]

The magnetic properties and interlayer distance d_{Fe} of the 15 ML Fe on 17 ML Fe_xMn_{1-x}/Cu(001) are categorized into three regimes as shown in Fig. 13. In regime (I), on Fe_xMn_{1-x}/Cu(001) with $x < 0.1$, the 15 ML Fe films are bcc structure [$d_{Fe} = 2.05$ Å referring to bcc(011)], and no exchange-bias coupling is observed. In regime (II), on Fe_xMn_{1-x}/Cu(001) with $0.1 < x < 0.35$, the Fe films are bcc structure with exchange-bias coupling. In regimes (III), on Fe_xMn_{1-x} with $x > 0.35$, the Fe films are single fcc phase [$d_{Fe} = 1.80$ Å referring to fcc(001)] without FM property, where no Kerr signal is observed in the temperature range 110–330 K under the field of 1600 Oe. No direct evidence indicates that the fcc Fe on 17 ML $Fe_{0.5}Mn_{0.5}$/Cu(001) is AF; see Ref. 34.
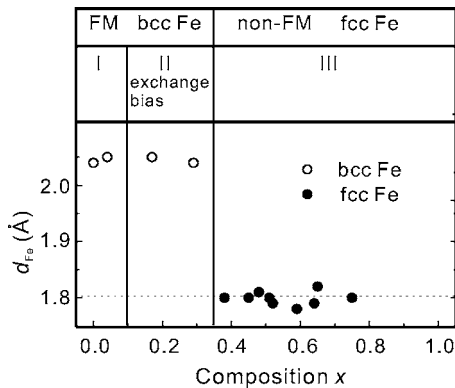

FIG. 13. Compositional dependence of the structural and magnetic phases for Fe/17 ML Fe_xMn_{1-x}/Cu(001). The Fe overlayer is either bcc (○) or fcc (●) affected by the Fe_xMn_{1-x} buffer layer with a critical composition of 0.35 that corresponds to d_{FeMn} of 1.85 Å. The upper panel indicates the magnetic phase of the Fe overlayer. (I) FM bcc Fe without exchange bias, (II) FM bcc Fe with exchange bias, and (III) non-FM fcc Fe.

IV. DISCUSSION

A. Stabilization of fcc Fe films on Fe_xMn_{1-x}/Cu(001)

The structure and magnetic properties of Fe films on Fe_xMn_{1-x}/Cu(001) are studied. Two significant results on the structure of Fe films by introducing the Fe_xMn_{1-x} layer are (a) the absence of fct structural phase near the Fe/Fe_xMn_{1-x} interphase and (b) thick fcc Fe films are obtained by introducing Fe_xMn_{1-x} with x near 0.5. We first discuss the effect of the lattice constant of Fe_xMn_{1-x}/Cu(001) and follow with the possibility of the intermixing at the Fe/Fe_xMn_{1-x} interphase.

The structural distinction between Fe films grown on Fe_xMn_{1-x}/Cu(001) and other substrates mentioned in Sec. I is that only the fcc phase is observed below the critical thickness. The fcc Fe films are stabilized without fcc-fct mixed phase by introducing the Fe_xMn_{1-x} layer. Considering the in-plane lattice constant, Fe_xMn_{1-x}/Cu(001) with x near 0.5 is compatible to the Cu(001) substrate as shown in Fig. 4. Additionally, the surface roughness of Fe_xMn_{1-x}/Cu(001) in this composition range is small according to the STM study as shown in Figs. 2(c)–2(e). However, the t_c of Fe films on 17 ML $Fe_{0.5}Mn_{0.5}$/Cu(001) is 25 ML (Fig. 7), which is much thicker than that of the Fe films on Cu(001) ($t_c = 10$ ML). It indicates that the contribution of Fe_xMn_{1-x} alloys to the Fe films on an Fe_xMn_{1-x}/Cu(001) system is doing more than just providing an fcc template. Note that the growth of the Fe at the initial stage on Fe_xMn_{1-x}/Cu(001) is very different from that on Cu(001).

The intermixing at the Fe/Fe_xMn_{1-x} interface would lead to an overestimation on the thickness of the fcc Fe layer, which could mislead our observation of the thick fcc Fe films. The interlayer atomic diffusion occuring at the Mn/Fe(001) interphase is reported, which leads to incorporation of Mn atoms into the Fe(001) substrate. The resulting layers at the interphase are found to be Mn/$Fe_{0.86}Mn_{0.14}$/$Fe_{0.96}Mn_{0.04}$/$Fe_{0.98}Mn_{0.02}$/Fe(001).[41] No evidence indicates that Mn atoms can diffuse into the fcc Fe, nor the atomic intermixing at the Fe/Fe_xMn_{1-x} interface. To investigate the intermixing at the Fe/Fe_xMn_{1-x} interface, an AES study on wedged Fe on 17 ML $Fe_{0.45}Mn_{0.55}$/Cu(001) and capped by 4.6 ML Fe was performed. The intensity ratio of peaks Mn_{542} and Fe_{702} as a function of thickness of Fe is shown in Fig. 14. The curve decays in an exponential fashion indicating the scattering of the Auger electrons of Mn atoms by the capping Fe layers. From the AES study, the intermixing occurring at Fe/Fe_xMn_{1-x} is not evident. Additionally, if the intermixing occurred, the diffusion of Mn atoms would be proportional to the composition of Mn in the Fe_xMn_{1-x} layer, i.e., $(1-x)$. However, the t_c does not increase with the Mn composition in the Fe_xMn_{1-x} layer as shown in Fig. 8. The intermixing at the Fe/Fe_xMn_{1-x} interface is excluded to be the factor that stabilizes the fcc structure of Fe films on Fe_xMn_{1-x}/Cu(001).

Another possible factor that contributes to the stabilization of the fcc Fe films is the roughness at the interface of Fe/Fe_xMn_{1-x}. The lattice misfit between Cu(001) and bulk Fe_xMn_{1-x} with $0.35 < x < 0.65$ is less than 1.1%, but up to 5.1% for the bulk Fe_xMn_{1-x} with $x < 0.35$ as shown in Fig. 4. The Fe_xMn_{1-x} films on Cu(001) with $x < 0.35$ are highly
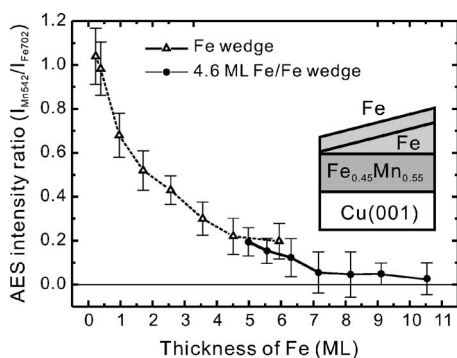
FIG. 14. AES intensity ratio of Mn 542 eV and Fe 702 eV as a function of the thickness of n ML Fe/17 ML $Fe_{0.45}Mn_{0.55}$/Cu(001). The films are capped by 4.6 ML Fe for obtaining the thicker range. The ratio demonstrates a pattern of exponential decay. It indicates no interlayer diffusion of Mn atoms from the $Fe_{0.45}Mn_{0.55}$ alloy to the top Fe layer.

strained, which may lead the Fe_xMn_{1-x} films to undergo stress relaxation by increasing the surface roughness as indicated by STM studies shown in Fig. 2. One can conclude that the roughness at the interface between Fe and Fe_xMn_{1-x}/Cu(001) plays a significant role in the stabilization of the top fcc Fe films.

B. Exchange bias of Fe films on Fe_xMn_{1-x}

bcc Fe films are found on the Fe_xMn_{1-x} buffer layer with $x < 0.35$ as shown in regimes (I) and (II) of Fig. 13. The exchange-bias coupling is found in regime (II) $(0.1 < x < 0.35)$; but not in regime (I) $(x < 0.1)$. We discuss the discrepancy in terms of Néel temperature (T_N) and the AF configuration of the Fe_xMn_{1-x}/Cu(001) underlayer.

The H_c in regime (I) is about 12 Oe at 150 K, which agrees with the H_c of 15 Oe for the 13 ML Fe/Cu(001) at 100 K.[42] The absence of exchange-bias coupling could be ascribed to the fact that the T_N for 17 ML Fe_xMn_{1-x}/Cu(001) with $x < 0.1$ is below the temperature range investigated (100–300 K) and that an ordered AF coupling is not established by the field-cooling procedure. It is feasible to estimate the T_N of 17 ML Fe_xMn_{1-x}/Cu(001) by the T_N of the bulk alloy with equivalent composition. For bulk Fe_xMn_{1-x} alloys with $x < 0.3$, the T_N decreases from 480 to 400 K with increasing x in a roughly monotonic fashion. For bulk $Fe_{0.2}Mn_{0.8}$ and $Fe_{0.3}Mn_{0.7}$, the T_N is about 430 and 375 K, respectively.[24] The T_b for 15 ML Fe/17 ML Fe_xMn_{1-x}/Cu(001) with $x = 0.2$ and 0.3 is 270 and 250 K. There is a difference of approximately 140 K. For bulk $Fe_{0.1}Mn_{0.9}$, the T_N is about 460 K.[24] The T_N for 17 ML Fe_xMn_{1-x}/Cu(001) in regime (I) can be estimated as 300–335 K, whereas no exchange bias is found. We con-

clude that the absence of the exchange bias coupling in regime (I) is not due to the low T_N of the alloys.

For bulk Fe_xMn_{1-x} with $x < 0.35$, the AF configuration is proposed to be colinear and aligns along the long axis of the fct structure.[24] The structure of 17 ML Fe_xMn_{1-x}/Cu(001) with $x < 0.1$ is fct $(c/a \sim 1.08$, as shown in Fig. 4) with the long axis perpendicular to the surface. It is feasible to propose that the AF anisotropy is also aligned along the out-of-plane orientation that is perpendicular to the in-plane easy axis of the Fe films. This perpendicular alignment may reduce the exchange-bias coupling.[39,44] Note that no out-of-plane magnetic signal is observed. Exchange-bias coupling is found in the Fe films on 17 ML Fe_xMn_{1-x}/Cu(001) with $0.1 < x < 0.35$ as shown in regime (II) of Fig. 13. In this regime, the c/a ratio in 17 ML Fe_xMn_{1-x}/Cu(001) is nearly 1.03, as shown in Fig. 4, which is more cubic than that in regime (I). Thus it might lead the exchange-bias coupling in the in-plane orientation observable.

Some studies on FM/AF with uncompensated AF layered systems reported that the H_{ex} decreases with increasing the interface roughness.[39] This seems to be plausible to our results since the surface roughness of Fe_xMn_{1-x}/Cu(001) in regime (I) is larger than that of regime (II). Note that the argument is applicable to the systems with uncompensated AF layer that the roughness reduces the total number of spins pinning the FM in one direction.[39] The AF configuration of the Fe_xMn_{1-x}/Cu(001) in our system should be compensated according to the bulk configuration.[24] Thus the rougher interface at Fe/Fe_xMn_{1-x} in regime (I) may lead to the absence of the exchange bias.

V. CONCLUSION

By varying the composition x of the Fe/Fe_xMn_{1-x}/Cu(001) bilayer system, a single fcc structural phase corresponding to non-FM property Fe films is constructed. The composition x of the Fe_xMn_{1-x} bottom layer affects the surface roughness that leads to the changes of the critical thickness t_c for the fcc-bcc structural phase transition of the Fe overlayer. Additionally, the magnetic properties of the bcc Fe/Fe_xMn_{1-x}/Cu(001) films, with or without exchange bias and the temperature-dependent behaviors, are correlated to the composition x, which might be due to the compositional dependence of the AF configuration of the Fe_xMn_{1-x} bottom layer. In a FM/AF bilayer system, the study reveals a method to manipulate the structure and magnetic property of the FM films by varying the composition of the AF alloy layer.

*Electronic address: weipane@gmail.com

†Author to whom correspondence should be addressed. Electronic address: mtlin@phys.ntu.edu.tw

[1] M.-T. Lin, C. H. Ho, C.-R. Chang, and Y. D. Yao, Phys. Rev. B **63**, 100404(R) (2001).

[2] A. M. N. Niklasson, B. Johansson, and H. L. Skriver, Phys. Rev. B **59**, 6373 (1999).

[3] S. Blügel, Appl. Phys. A: Mater. Sci. Process. **63**, 595 (1996).

[4] M.-T. Lin, C. H. Ho, C.-R. Chang, and Y. D. Yao, J. Appl. Phys. **89**, 1 (2001).

[5] W. C. Lin, C. C. Kuo, C. L. Chiu, and M.-T. Lin, Surf. Sci. **478**, 9 (2001).

[6] D. Qian, X. F. Jin, J. Barthel, M. Klaua, and J. Kirschner, Phys. Rev. Lett. **87**, 227204 (2001).

[7] D. Spišák and J. Hafner, Phys. Rev. B **66**, 052417 (2002).

[8] D. Li, M. Freitag, J. Pearson, Z. Q. Qiu, and S. D. Bader, Phys. Rev. Lett. **72**, 3112 (1994).

[9] D. Li, M. Freitag, J. Pearson, Z. Q. Qiu, and S. D. Bader, J. Appl. Phys. **76**, 6425 (1994).

[10] S. Müller, P. Bayer, C. Reischl, K. Heinz, B. Feldmann, H. Zillgen, and M. Wuttig, Phys. Rev. Lett. **74**, 765 (1995).

[11] M. Zharnikov, A. Dittschar, W. Kuch, C. M. Schneider, and J. Kirschner, Phys. Rev. Lett. **76**, 4620 (1996).

[12] D. Spišák and J. Hafner, Phys. Rev. B **64**, 205422 (2001).

[13] M. Friák, M. Šob, and V. Vitek, Phys. Rev. B **63**, 052405 (2001).

[14] D. Spišák and J. Hafner, Phys. Rev. Lett. **88**, 056101 (2002); with the erratum D. Spišák and J. Hafner, Phys. Rev. Lett. **88**, 239903(E) (2002).

[15] T. Gutjahr-Löser, D. Sander, and J. Kirschner, J. Appl. Phys. **87**, 5920 (2000).

[16] W. L. O'Brien and B. P. Tonner, Phys. Rev. B **51**, 617 (1995).

[17] M.-T. Lin, J. Shen, W. Kuch, H. Jenniches, M. Klaua, C. M. Schneider, and J. Kirschner, Phys. Rev. B **55**, 5886 (1997).

[18] S. S. Kang, W. Kuch, and J. Kirschner, Phys. Rev. B **63**, 024401 (2000).

[19] M. D. Martins, L. H. F. Andrade, P. L. Gastelois, and W. A. A. Macedo, J. Appl. Phys. **89**, 6680 (2001).

[20] R. Thamankar, S. Bhagwat, and F. O. Schumann, Phys. Rev. B **69**, 054419 (2004).

[21] A. Biedermann, R. Tscheliessnig, M. Schmid, and P. Varga, Phys. Rev. Lett. **87**, 086103 (2001).

[22] A. Biedermann, M. Schmid, and P. Varga, Phys. Rev. Lett. **86**, 464 (2001).

[23] B. Gubanka, M. Donath, and F. Passek, Phys. Rev. B **54**, R11153 (1996).

[24] Y. Endoh and Y. Ishikawa, J. Phys. Soc. Jpn. **30**, 1614 (1971).

[25] M. Podgórny, Phys. Rev. B **45**, 797 (1992).

[26] S. J. Kennedy and T. J. Hicks, J. Magn. Magn. Mater. **81**, 56 (1989).

[27] D. Spišák and J. Hafner, Phys. Rev. B **61**, 11569 (2000).

[28] F. Offi, W. Kuch, and J. Kirschner, Phys. Rev. B **66**, 064419 (2002).

[29] W. Kuch, L. I. Chelaru, F. Offi, J. Wang, M. Kotsugi, and J. Kirschner, Phys. Rev. Lett. **92**, 017201 (2004).

[30] R. Thamankar, S. Bhagwat, and F. O. Schumann, Phys. Rev. B **69**, 054411 (2004).

[31] J. Wang, W. Kuch, L. I. Chelaru, F. Offi, and M. Kotsugi, Appl. Phys. Lett. **86**, 122504 (2005).

[32] A. Dittschar, M. Zharnikov, W. Kuch, M.-T. Lin, C. M. Schneider, and J. Kirschner, Phys. Rev. B **57**, R3209 (1998).

[33] M.-T. Lin, W. C. Lin, C. C. Kuo, and C. L. Chiu, Phys. Rev. B **62**, 14268 (2000). The evaporation rate for Fe, Co, and Ni, monitored by MEED, thus can be in this way precisely controlled with an accuracy of 0.05 ML for a deposition coverage of 10 ML, which is corresponding to a composition accuracy of 0.01.

[34] C. C. Kuo, W. Pan, Y. C. Chen, and M.-T. Lin, J. Appl. Phys. **93**, 8743 (2003).

[35] M.-T. Lin, J. Shen, W. Kuch, H. Jenniches, M. Klaua, C. M. Schneider, and J. Kirschner, Surf. Sci. **410**, 290 (1998).

[36] W. Pan, D. Sander, M.-T. Lin, and J. Kirschner, Phys. Rev. B **68**, 224419 (2003).

[37] W. Pan, R. Popescu, H. L. Meyerheim, D. Sander, O. Robach, S. Ferrer, M.-T. Lin, and J. Kirschner, Phys. Rev. B **71**, 174439 (2005).

[38] J. Giergiel, J. Kirschner, J. Landgraf, J. Shen, and J. Woltersdorf, Surf. Sci. **310**, 1 (1994).

[39] J. Nogués and I. K. Schuller, J. Magn. Magn. Mater. **192**, 203 (1999).

[40] C. Leighton, J. Nogués, B. J. Jönsson-Åkerman, and I. K. Schuller, Phys. Rev. Lett. **84**, 3466 (2000).

[41] T. K. Yamada, M. M. Bischoff, T. Mizoguchi, and H. V. Kempen, Surf. Sci. **516**, 179 (2002).

[42] A. Berger, B. Feldmann, H. Zillgen, and M. Wuttig, J. Magn. Magn. Mater. **183**, 35 (1998).

[43] W. Pan, N.-Y. Jih, C.-C. Kuo, and M.-T. Lin, J. Appl. Phys. **95**, 7297 (2004).

[44] R. Jungblut, R. Coehoorn, M. T. Johnson, J. aan de Stegge, and A. Reinders, J. Appl. Phys. **75**, 6659 (1994).